ORGANIC LETTERS

2013
Vol. 15, No. 13
3400–3403

Aggregation Induced Emission Enhancement in Ionic Self-Assembled Aggregates of Benzimidazolium Based Cyclophane and Sodium Dodecylbenzenesulfonate

Sandeep Kumar,[†] Prabhpreet Singh,[†] Aman Mahajan,[‡] and Subodh Kumar*,[†]

Department of Chemistry, UGC Centre for Advanced Studies, Guru Nanak Dev University, Amritsar 143 005, India, and Department of Physics, Guru Nanak Dev University, Amritsar 143 005, India

subodh_gndu@yahoo.co.in

Received May 23, 2013

ABSTRACT

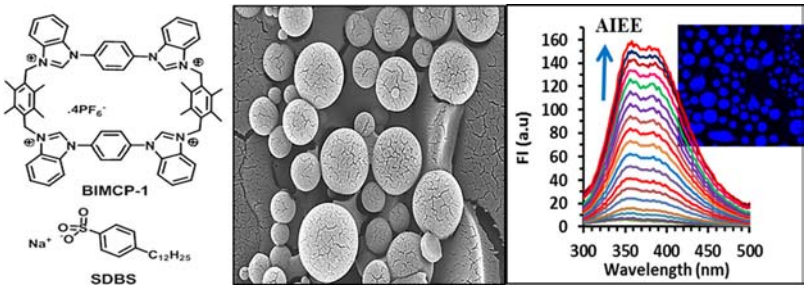

Cyclophane BIMCP-1 undergoes ionic self-assembly with surfactant sodium dodecylbenzenesulfonate (SDBS) at a concentration far below its CMC value to form aggregates with spherical morphology. The rotational restriction of rings in these aggregates facilitates 32-fold enhancement in emission intensity (AIEE) to allow fluorescence based determination of SDBS with 4 μM (1.4 ppm) as the lowest detection limit. Sodium salts of fatty acids and inorganic anions halides, CN^-, HSO_4^-, SO_4^{2-}, $H_2PO_4^-$, SCN^-, and NO_3^- do not interfere in the estimation of SDBS.

In light of the inspirations which natural processes[1] have provided us, the substantial advances in the design and fabrication of supramolecular assemblies have been achieved through a bottom-up approach by elegantly utilizing noncovalent interactions such as electrostatic, hydrophobic, van der Waals and hydrogen bonding, etc.[2,3]Among varied processes of self-assembly, the ionic self-assembly, i.e. the coupling of two structurally different building blocks through columbic interactions, has turned into a powerful tool to create new nanostructured chemical materials.[3] Various combinations between peptides, polyelectrolytes, surfactants, and extended rigid organic scaffolds could be employed for creating new materials via ionic self-assembly.[4] In such systems, though molecular recognition (space, size and complementarity) and columbic interactions between two oppositely charged components play a vital role in the initiation of ionic self-assembly process, the cooperative binding mechanism relying on weak interactions further propagates the final self-assembled structure.

Surfactants due to their amphiphilic nature are well-known to produce supramolecular aggregates such as

[†] Department of Chemistry.
[‡] Department of Physics.

(1) (a) Benyus, J. M. *Biomimicry: Innovation Inspired by Nature*; Quill-William Morrow: New York, 1997. (b) Branden, C.-I.; Tooze, J. *Introduction to Protein Structure*, 2nd ed.; Garland: New York, 1999. (c) Zhang, S. *Nat. Biotechnol.* **2003**, *21*, 1171.

(2) (a) Hoeben, F. J. M.; Jonkheijm, P. L.; Meijer, E. W.; Schenning, A. P. H. J. *Chem. Rev.* **2005**, *105*, 1491. (b) Wang, L.; Li, L. L.; Ma, H. L.; Wang, H. *Chin. Chem. Lett.* **2013**, *24*, 351.

(3) (a) Faul, C. F. J.; Antonietti, M. *Adv. Mater.* **2003**, *15*, 673. (b) Greaves, T. L.; Drummond, C. J. *Chem. Soc. Rev.* **2008**, *37*, 1709. (c) Rehm, T. H.; Schmuck, C. *Chem. Soc. Rev.* **2010**, *39*, 3597. (d) Thomas, J. A. *Dalton Trans.* **2011**, *40*, 12005. (e) Greaves, T. L.; Drummond, C. J. *Chem. Soc. Rev.* **2013**, *42*, 1096.

(4) (a) Cheng, Z. Y.; Ren, B. Y.; Chang, X. Y.; Liu, R.; Tong, Z. *Chin. Chem. Lett.* **2012**, *23*, 619. (b) Ma, T. Y.; Li, H.; Deng, Q. F.; Liu, L.; Ren, T. Z.; Yuan, Z. Y. *Chem. Mater.* **2012**, *24*, 2253. (c) Lv, C.; Xu, G.; Chen, X. *Chem. Lett.* **2012**, *41*, 1201. (d) Percebom, A. M.; Janiak, J.; Schillén, K.; Piculell, L.; Loh, W. *Soft Matter* **2013**, *9*, 515. (e) Guo, Y. N.; Li, Y.; Zhi, B.; Zhang, D.; Liu, Y.; Huo, Q. *RSC Adv.* **2012**, *2*, 5424. (f) Chen, L. G.; Bermudez, H. *Langmuir* **2012**, *28*, 1157. (g) de-Rooy, S. L.; Das, S.; Li, M.; El-Zahab, B.; Jordan, A.; Lodes, R.; Weber, A.; Chandler, L.; Baker, G. A.; Warner, I. M. *J. Phys. Chem. C* **2012**, *116*, 8251.

10.1021/ol401452t
Published on Web 06/20/2013

micelles and vesicles in aqueous solution.[5] The coupling of anionic surfactants and other sulfonates with cationic motifs viz. ammonium, pyridinium, anilinium, etc. has resulted in the formation of many ordered ionic self-assemblies.[6] As the self-assembly of two components is highly dependent on the components' structure, even a small structural change can put the self-assembling process into total disarray. So, the recognition of stimuli based on the self-assembly process provides higher selectivity over simple equilibrium based processes.[7]

Molecular architectures possessing imidazolium and its benzo derivatives as motifs have been used for the recognition of anions primarily through electrostatic interactions between the positively charged imidazolium moiety and the target anion.[8] The imidazolium based cyclophanes, due to their high degree of structural rigidity and predefined cavity size, have further shown energetically favored encapsulation of guest molecules including anions, cations, and neutral molecules.[9] The recognition process in such systems is usually associated with the change in the fluorescence intensity and/or shift in emission maxima due to various photophysical processes taking place between two components. Recently, Sessler et al. have reported that a large imidazolium based tetracationic cyclophane can adjust its shape and conformation to accommodate anionic guests of different sizes and charges within its central core and promotes the formation of different macromolecular aggregates.[10]

Herein, we report benzimidazolium based tetracationic cyclophane **BIMCP-1** which on addition of SDBS (sodium dodecylbenzenesulfonate, $< 25\ \mu$M) far below its CMC value (1.5 mM) leads to the formation of the ionic self-assembling process to provide aggregates with spherical morphology of a 1−1.5 μm diameter, as observed from SEM and confocal images of their thin films. This aggregation process is also associated with aggregation induced emission enhancement (AIEE) to enable fluorescence based determination of SDBS. The confocal images of these films also confirm that the aggregation is associated with an increase in the emission intensity. Interestingly, this ionic self-assembling process is also initiated by sodium dodecyl sulfate (SDS) but long chain fatty carboxylic acids or lower homologues of SDS/SDBS do not induce such assembly or cause any change in the fluorescence intensity of **BIMCP-1**. This recognition of SDBS/SDS is based on both columbic interactions of the binding site (SO_3^-/OSO_3^-) and the hydrophobic effect of the long alkyl chain. The low fluorescence enhancement in the case of acyclic analog **2** also points to the significance of the cyclic structure in **BIMCP-1** in the aggregation and recognition process.

Scheme 1. Synthesis of Cyclophane **BIMCP- 1** and Its Acyclic Analog **2**

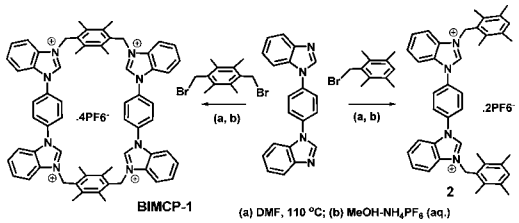

The target benzimidazolium based cyclophane **BIMCP-1** and its acyclic analog **2** were synthesized by alkylation of 1,4-bis(benzimidazol-1-yl)benzene with 1,4-bis(bromomethyl)-2,3,5,6- and 3-bromomethyl-1,2,4,5-tetramethylbenzene, respectively (Scheme 1). All the compounds were thoroughly characterized by the usual spectroscopic techniques viz. ^{1}H NMR, ^{13}C NMR, HRMS, and CHN analysis (Supporting Information Figure SI-1−6).

To evaluate the aggregation behavior, the thin films of **BIMCP-1** (10 μM) and its 1:2 solutions with SDBS/SDS (2 equiv) in aqueous solution (5% DMSO) were prepared on the glass surface using the drop cast method. The respective films of **BIMCP-1** alone do not show any morphology under both confocal microscopy and SEM. The films of **BIMCP-1** and SDBS exhibit spherical structures with diameters = 0.4−1.2 μm (Figure 1a). Enlargement under SEM show these spheres to be formed by the aggregation of fiberlike structures (Figure 4). Under confocal microscopy, these films show circular aggregates 0.5−1.5 μm in size (Figure 1c), which are in consonance with the SEM image. AFM images of these films are also in consonance with the formation spherical morphology (Figure SI-7). Also under confocal, these spheres appear intense blue in comparison to the almost nonfluorescent film of **BIMCP-1** alone (Figure SI-8). The intense blue fluorescence is in consonance with 32-fold increase in fluorescence intensity on addition of SDBS to the solution of **BIMCP-1**. In the

(5) (a) Rosoff, M., Ed. *Vesicles*; Dekker: New York, 1996. (b) Carmona-Ribeiro, A. M. *Chem. Soc. Rev.* **1992**, *21*, 209.

(6) (a) Cortez, M. L.; Pallarola, D.; Ceolín, M.; Azzaroni, O.; Battaglini, F. *Chem. Commun.* **2012**, *48*, 10868. (b) Evans, R. C.; Knaapila, M.; Willis-Fox, N.; Kraft, M.; Terry, A.; Burrows, H. D.; Scherf, U. *Langmuir* **2012**, *28*, 12348. (c) Li, Y.; Zhang, D.; Gai, F.; Zhu, X.; Guo, Y.; Ma, T.; Liu, Y.; Huo, Q. *Chem. Commun.* **2012**, *48*, 7946. (d) Ahmed, R.; Priimagi, A.; Faul, C. F. J.; Manners, I. *Adv. Mater.* **2012**, *24*, 926. (e) Zhao, M.; Zhao, Y.; Zheng, L.; Dai, C. *Chem.—Eur. J.* **2013**, *19*, 1076. (f) Choudhury, S. D.; Bhasikuttan, A. C.; Pal, H.; Mohanty, J. *Langmuir* **2011**, *27*, 12312.

(7) (a) Kumar, M.; Jonnalagadda, N.; George, S. J. *Chem. Commun.* **2012**, *48*, 10948. (b) Xin, Y.; Kong, X.; Zhang, X.; Lv, Z.; Du, X. *Langmuir* **2012**, *28*, 11153. (c) Harada, A.; Kobayashi, R.; Takashima, Y.; Hashidzume, A.; Yamaguchi, H. *Nat. Chem.* **2011**, *3*, 34. (d) Faul, C. F. J.; Krattiger, P.; Smarsly, B. M.; Wennemers, H. *J. Mater. Chem.* **2008**, *18*, 2962.

(8) (a) Xu, Z.; Chen, X.; Kim, H. N.; Yoon, J. *Chem. Soc. Rev.* **2010**, *39*, 127. (b) Yoon, J.; Kim, S. K.; Singh, N. J.; Kim, K. S. *Chem. Soc. Rev.* **2006**, *35*, 355.

(9) (a) Serpell, C. J.; Cookson, J.; Thompson, A. L.; Beer, P. D. *Chem. Sci.* **2011**, *2*, 494. (b) Shirinfar, B.; Ahmed, N.; Park, Y. S.; Cho, G. S.; Youn, S.; Han, J. K.; Nam, H. G.; Kim, K. S. *J. Am. Chem. Soc.* **2013**, *135*, 90. (c) Ahmed, N.; Shirinfar, B.; Youn, I. S.; Bist, A.; Suresh, V.; Kim, K. S. *Chem. Commun.* **2012**, *48*, 2662. (d) Guo, Z.; Song, N. R.; Moon, J. H.; Kim, M.; Jun, E. J.; Choi, J.; Lee, J. Y.; Bielawski, C. W.; Sessler, J. L.; Yoon, J. *J. Am. Chem. Soc.* **2012**, *134*, 17846. (e) Chun, Y.; Singh, N. J.; Hwang, I. C.; Lee, J. W.; Yu, S. U.; Kim, K. S. *Nat. Commun.* **2013**, *4*, 1797. (f) Chellappan, K.; Singh, N. J.; Hwang, I. C.; Lee, J. W.; Kim, K. S. *Angew. Chem., Int. Ed.* **2005**, *44*, 2899.

(10) (a) Rambo, B. M.; Gong, H. Y.; Oh, M.; Sessler, J. L. *Acc. Chem. Res.* **2012**, *45*, 1390. (b) Gong, H. Y.; Rambo, B. M.; Lynch, V. M.; Keller, K. M.; Sessler, J. L. *Chem.—Eur. J.* **2012**, *18*, 7803. (c) Gong, H. Y.; Rambo, B. M.; Nelson, C. A.; Cho, W.; Lynch, V. M.; Zhu, X.; Oh, M.; Sessler, J. L. *Dalton Trans.* **2012**, *41*, 1134. (d) Gong, H. Y.; Rambo, B. M.; Nelson, C. A.; Cho, W.; Lynch, V. M.; Zhu, X.; Oh, M.; Sessler, J. L. *Chem. Commun.* **2011**, *47*, 5973. (e) Gong, H. Y.; Rambo, B. M.; Karnas, E.; Lynch, V. M.; Keller, K. M.; Sessler, J. L. *J. Am. Chem. Soc.* **2011**, *133*, 1526.

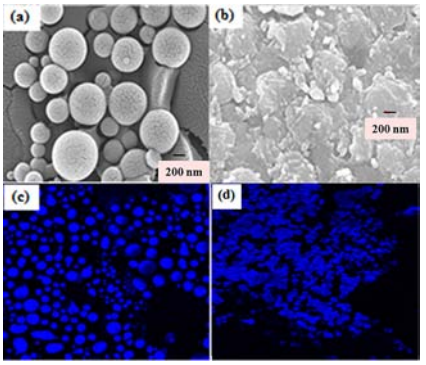

Figure 1. SEM (a−b) and confocal (c−d) images, respectively, of **BIMCP-1** with different surfactants; (a,c) **BIMCP-1** + SDBS; (b,d) **BIMCP-1** + SDS.

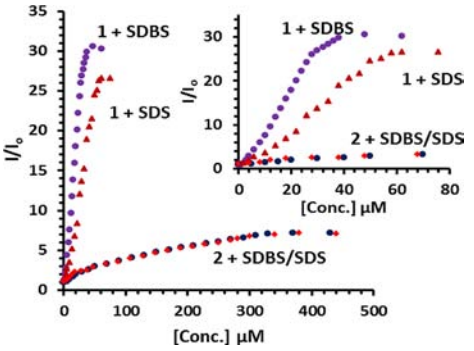

Figure 2. Plot of fluorescence intensity (I/I_o) vs concentration of SDBS and SDS for **BIMCP-1** and **2** in water (5% DMSO) [Inset: shows selectivity of **BIMCP-1** with SDBS/SDS in comparison to open analog **2**].

case of SDS, hemispheres 10−15 μm in size are formed by aggregation of **BIMCP-1** with SDS (Figure 1b, d) and exhibit increased luminescence under confocal microscopy. Dynamic light scattering experiments of **BIMCP-1**/SDS and **BIMCP-1**/SDBS (1:2) complexes at 5 μM show the formation of aggregates with 100−1000 nm sizes and are in agreement with aggregation of **BIMCP-1** with SDS and SDBS under fluorescence experimental conditions (Figure SI-9).

The UV−vis spectra of **BIMCP-1** and **2** in H_2O (5% DMSO) exhibit the absorption maxima at 265 nm (±5 nm). On excitation at 270 nm, the solutions of both **BIMCP-1** and **2** exhibit two emission maxima at 360 and 385 nm and display a linear increase in the fluorescence intensity between 1 and 50 μM and point to the absence of aggregation or any intramolecular interaction in various components of **BIMCP-1** (Figure SI-10). The addition of SDBS and SDS (50 μM) to the solution of **BIMCP-1** (2 μM) in H_2O (5% DMSO) leads to respectively a 32- and 27-fold increase in emission intensity at 360 and 380 nm. The acyclic analog **2** exhibits only ∼3-fold emission intensity enhancement on addition of 50 μM SDS and SDBS and ∼7-fold emission intensity enhancement at > 400 μM SDBS and SDS (Figure 2). Remarkably, the sodium salts of long chain carboxylates such as laurate, myristate, palmitate, and stearate (100 μM each) cause a < 1-fold increase in the emission intensity of **BIMCP-1** and **2**, whereas the addition of methyl sulfonate, butyl sulfonate, octyl sulfonate, decyl sulfonate, octyl sulfate, decyl sulfate, etc. or inorganic anions viz. halides, $H_2PO_4^-$, CN^-, SCN^-, HSO_4^-, SO_4^{2-} (100 μM each), etc. causes an insignificant change in both the absorption and emission spectrum of **BIMCP-1** and **2** (Figure SI-11). Thus, **BIMCP-1** shows remarkably high sensitivity toward SDBS and SDS.

Temperature dependent fluorescence titrations reveal that the formation of aggregates between **BIMCP-1** and surfactants, which are responsible for AIEE phenomena, is fully reversible. On increasing the temperature of the solution of **BIMCP-1** (2 μM) and SDBS/SDS (50 μM) from 25 to 85 °C, the fluorescence emission intensity of the solution decreases ∼7-fold, which is recovered after cooling the solution back to 25 °C (Figure SI-12). This could be attributed to the occurrence of deaggregation and aggregation processes respectively on increasing and decreasing the temperature of the solution. Furthermore, the ^{1}H NMR spectrum of **BIMCP-1** (2.5 mM), in CD_3CN/D_2O (1:1), on addition of 2 equiv of SDBS exhibits an upfield shift of the singlet due to *p*-phenylene protons by 0.27 ppm (from δ 7.96 to 7.69) (Figure SI-13). Upon reverse ^{1}H NMR titration, i.e. addition of **BIMCP-1** to a 2.5 mM solution of SDBS, the aryl protons of the SDBS molecule at δ 7.73 and 7.31 were upfield shifted to δ 7.63 and 7.25 revealing aromatic $\pi-\pi$ interactions between **BIMCP-1** and SDBS (Figure SI-14,15).

It could be attributed that the surfactant SDBS binds strongly with **BIMCP-1** through electrostatic interactions between oppositely charged **BIMCP-1** and a sulfonate moiety of the surfactant along with some $\pi-\pi$ interactions between the phenyl ring of the SDBS and phenylene core of **BIMCP-1** to produce *ionic self-assembled* aggregates. The lifetime measurement of the excited state of **BIMCP-1** in the presence of ≥2 equiv of SDBS or SDS shows an increase in lifetime from 0.76 to 8.9 ns. The plot of the concentration of the **BIMCP-1**/SDBS complex vs K_f and K_{nr} shows a respective increase and decrease in the values. Therefore, both the increase in fluorescence of the **BIMCP-1**/SDBS complex and decrease in the deactivation of the excited state through nonradiative processes due to restricted rotation of the aryl rings in these aggregates contribute to the overall emission enhancement (Figure SI-16−19).

SDBS and SDS are widely used surfactants in domestic and industrial formulations, and their presence in natural waters arouses concern for human health and the global ecosystem.[11] Several techniques are currently used to

(11) (a) Chen, B.; Wang, S.; Zhang, Q.; Huang, Y. *Analyst* **2012**, *137*, 1232. (b) Perales, J. A.; Manzano, M. A.; Sales, D.; Quiroga, J. M. *Bull. Environ. Contam. Toxicol.* **1999**, *63*, 94. (c) Palazzesi, F.; Calvaresi, M.; Zerbetto, F. *Soft Matter* **2011**, *7*, 9148. (d) Brandt, K. K.; Hesselsøe, M.; Roslev, P.; Henriksen, K.; Sørensen, J. *Appl. Environ. Microbiol.* **2001**, *67*, 2489. (e) Urakawa, H.; Inaba, K.; Tsuneda, S. *FEMS Microbiol. Lett.* **2008**, *282*, 166.

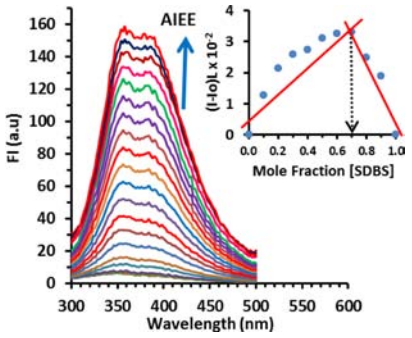

Figure 3. Effect of gradual addition of SDBS on the emission spectrum of **BIMCP-1** (2 μM) in water (5% DMSO) [Inset: Job's plot of **BIMCP-1** with SDBS shows 1:2 (**BIMCP-1**/SDBS) stoichiometry].

detect SDBS, SDS, and their homologues.[12] However, fluorescent probes are considered to be more sensitive and specific, possessing potential in regards to portability and real time monitoring with a fast response time.[13] To demonstrate the practical utility of the present fluorescence turn-on assay for the detection of surfactants, detailed fluorescence titrations have been carried out. The gradual addition of aliquots of SDBS to the solution of **BIMCP-1** (2 μM) in water (5% DMSO) shows a gradual increase in fluorescence intensity and achieves a plateau after addition of 50 μM (25 equiv) of SDBS (Figure 3). Similarly, the addition of SDS to the solution of **BIMCP-1** results in a 27-fold increase in emission intensity at 50 μM and then achieves a plateau (Figure SI-20). The lowest detection limit for both SDBS and SDS is 4.0 μM (1.4 ppm). The nonlinear regression analysis of these titration data using SPECFIT-32 shows the formation of 1:2 (**BIMCP-1**/SDBS or **BIMCP-1**/SDS) stoichiometric complexes with stability constant (log β) values of 9.11 $\pm$ 0.04 and 8.61 $\pm$ 0.02, respectively. The Job plot of **BIMCP-1** with both SDBS and SDS shows an inflection point near 0.7 and further confirms the formation of a 1:2 (**BIMCP-1**:SDBS/SDS) stoichiometric complex (Figure 3, Inset, SI-21).

On the other hand, the acyclic analog **2** (5 μM, water (5% DMSO) on addition of SDBS or SDS exhibits a much smaller increase in the emission intensity at 352 and 385 nm and achieves a plateau after addition of 400 μM of SDBS/SDS. The spectral fitting of these titration data shows the formation of a mixture of 1:1 and 1:2 stoichiometric species (**2**:SDBS/SDS) with relatively lower

(12) (a) Hu, Y. Y.; He, Y. Z.; Qian, L. L. *Anal. Chim. Acta* **2005**, *536*, 251. (b) Villar, M.; Callejon, M.; Jimenez, J. C.; Alonso, E.; Guiraum, A. *Anal. Chim. Acta* **2007**, *599*, 92. (c) Moldovan, Z.; Avram, V.; Marincas, O.; Petrov, P.; Ternes, T. *J. Chromatogr., A* **2011**, *1218*, 343. (d) Akyuz, M. *Talanta* **2007**, *71*, 471. (e) Kumar, S.; Arora, S.; Singh, P.; Kumar, S. *RSC Adv.* **2012**, *2*, 9969.

(13) (a) Kikuchi, K. *Chem. Soc. Rev.* **2010**, *39*, 2048. (b) Yang, Y.; Zhao, Q.; Feng, W.; Li, F. *Chem. Rev.* **2013**, *113*, 192. (c) Moragues, M.; Martínez-Máñez, E. R.; Sancenón, F. *Chem. Soc. Rev.* **2011**, *40*, 2593. (d) Wu, J.; Liu, W.; Ge, J.; Zhang, H.; Wang, P. *Chem. Soc. Rev.* **2011**, *40*, 3483. (e) Du, J.; Hu, M.; Fan, J.; Peng, X. *Chem. Soc. Rev.* **2012**, *41*, 4511.

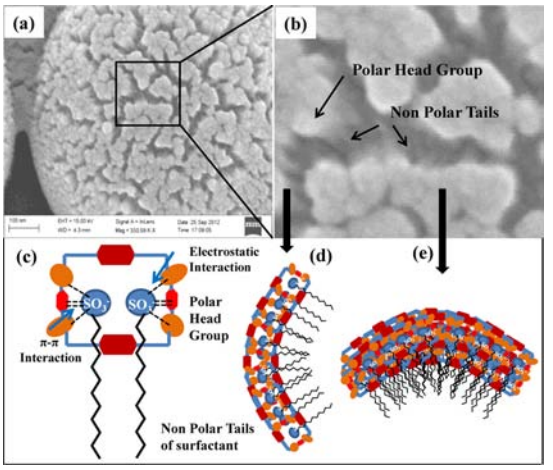

Figure 4. Proposed model for the formation of spherical aggregates. (a) **BIMCP-1** + SDBS; (b) part of Figure 4a after enlarging; (c) model for encapsulation of the anionic surfactant showing electrostatic/$\pi-\pi$ interaction with hydrophobic tails extending outside for stabilization; (d) lateral view of Figure 4b; (e) top to bottom view of Figure 4b.

binding constant values than those observed for **BIMCP-1** (Figure SI-22−23).

We propose that the mechanism for the observation of these fine spherical morphologies for the **BIMCP-1**/SDBS complex is related to micelle type aggregation (Figure 4). In polar solvent (H_2O), the complexes of benzimidazolium moieties of **BIMCP-1** with sulfonate groups are present on the outside surface of the aggregates to form the hydrophilic exterior, whereas the dodecyl chains (hydrophobic tails) tend to gather in the core to stabilize the aggregates and result in aggregation induced fluorescence enhancement. The encapsulation of the anionic surfactant molecules in the cyclophane cavity largely neutralizes the positive charge of **BIMCP-1**, reduces the repulsive electrostatic interactions among the molecules of **BIMCP-1**, and in turn facilitates the aggregation process.

In conclusion, the cyclophane **BIMCP-1** in the presence of <25 equiv of (1−50 μM) SDBS/SDS undergoes aggregation induced emission enhancement well below their CMC values and allows fluorescence based determination of SDS/SDBS. Confocal imaging and SEM studies confirm the formation of aggregates.

Acknowledgment. We thank DST, New Delhi for financial assistance under the FIST program; CSIR, New Delhi for a fellowship to Sandeep Kumar; and UGC, New Delhi under the CAS program.

Supporting Information Available. Experimental procedures, additional fluorescence/UV−vis data, HRMS, and ^{1}H NMR titrations are available. This material is available free of charge via the Internet at http://pubs.acs.org.

The authors declare no competing financial interest.